On-orbit Microwave Blackbody Calibration Using Regions of Dense Vegetation

Shannon Brown and Chris Ruf
University of Michigan
Ann Arbor, MI

I. INTRODUCTION

Satellite microwave radiometers have provided measurements of the vertical temperature distribution, cloud liquid water, radiometric path delay, sea ice concentration, precipitation, and various other geo-physical parameters for over 30 years [1]. Microwave radiometers take measurements of the apparent brightness temperature (TB) of a scene at various frequencies in order to retrieve atmospheric parameters. Accurate retrieval of these parameters requires a precise inversion algorithm and a well calibrated instrument.

Radiometers are calibrated on-orbit by comparing the measured brightness temperatures to on-Earth targets whose brightness temperature is known or can be accurately modeled. The dynamic range of brightness temperatures that an Earth observing radiometer will encounter is approximately 120 K – 310 K from 18 – 40 GHz and 0 – 55^o incidence. The brightness temperatures must be calibrated accurately at both ends of the TB spectrum. A method developed by [2], which isolates a statistical lower bound for brightness temperature over the ocean, can be used to calibrate the TBs at the cold end of the spectrum. There remains a need for a stable on-Earth hot calibration reference target. An ideal target would be a large isothermal blackbody in the field of view of the Earth pointing antenna. Heavily vegetated regions of the Amazon rainforest can be treated as pseudo-blackbodies due to the emission of the canopy being independent of polarization and incidence angle. With a known surface emission, SSM/I TBs can be used to determine a hot calibration reference for frequencies from 18 – 40 GHz and incidence angles of 0 to 55^o. Having this provides a calibration reference for any radiometer operating within that range.

II. METHODOLOGY

The brightness temperature of a vegetation canopy over a soil surface is a function of the emission from the soil surface and the vegetation layer [3]. This can be modeled as

$$T_{B,canopy}(f,\theta,p) = \left(\frac{1-\Gamma_s(f,\theta,p)}{L(f,\theta)}\right)\left(1-\frac{1}{L(f,\theta)}\right)\times (1-a(f))T_v + \left(\frac{1-\Gamma_s(f,\theta,p)}{L(f,\theta)}\right)T_s \quad (1)$$

where

$\Gamma_s(f, \theta, p)$	*soil-vegetation reflectivity,*
$L(f, \theta)$	*loss factor of the vegetation canopy,*
$a(f)$	*single scattering albedo of the canopy,*
T_v	*physical temperature of the canopy,*
T_s	*physical temperature of the surface.*

At frequencies greater than 10 GHz with a dense canopy that has high moisture content, the optical depth becomes very large and the transmissivity (inverse of the loss factor) of the canopy approaches zero. In this case the brightness temperature of the canopy reduces to,

$$T_{B,canopy} = (1-a(f))T_v, \quad (2)$$

where the single scattering albedo is isotropic and independent of polarization. It is reasonable to assume that the albedo varies with frequency since the wavelength of the radiation is changing relative to the leaf dimensions. Using this model as the surface contribution, the radiative transfer equation is written as

$$TB_{app}(f,\theta) = (1-a(f))T_v e^{-\tau(f)\sec(\theta)} + TB_{up}(f,\theta) + \Gamma_{scat}(f)(TB_{down}(f))e^{-\tau(f)\sec(\theta)} \quad (3)$$

where

θ *incidence angle,*

$\Gamma_{scat}(f)$ *represents the fraction of downwelling radiation scattered into θ from the canopy,*

$TB_{down}(f)$ *represents the hemispherical contribution of the downwelling brightness temperature,*

$TB_{UP}(f,\theta)$ *upwelling atmospheric brightness temperature,*

TB_{app} *main beam brightness temperature at the antenna,*

$\tau(f)$ *optical depth of the atmosphere.*

The surface contribution can be estimated from SSM/I brightness temperatures by inverting (3) and solving for T_v. This requires that $TB_{UP}(f,\theta)$, $\tau(f)$, $TB_{down}(f)$, $\Gamma_{scat}(f)$, and $a(f)$ are known for SSM/I frequencies. These variables can be estimated from the SSM/I data.

Statistical inversion methods have been used to retrieve atmospheric parameters such as vertically integrated path delay and liquid water [4]. A similar method is used to find the upwelling TBs. The upwelling brightness temperature at SSM/I frequencies is estimated using a statistical inversion involving the 19.35, 22.235, and 37.0 GHz SSM/I channels. The upwelling TB is written as a linear combination of the lower three channels,

$$TB_{up}(f,53^o) = c_0 + c_1 TB_{app}(19.35,53^o) + c_2 TB_{app}(22.235,53^o) + c_3 TB_{app}(37.0,53^o) \quad (4)$$

Using an average atmospheric effective radiating temperature over the Amazon and the SSM/I upwelling TBs determined from (4) [5], the integrated optical depth can be determined by

$$\tau(f) = -\ln\left(1 - \frac{TB_{up}(f,\theta)}{T_{eff}(f)}\right)\cos(\theta) \quad (5)$$

The hemispherical downwelling component is the downwelling brightness temperature from the atmosphere and the cosmic background integrated over solid angle. This can be estimated at each SSM/I frequency from the upwelling TB component by

$$TB_{down}(f) = c_0 + c_1 TB_{up}(f,53^o) \quad (6)$$

The hemispherical downwelling radiation is assumed to be scattered isotropically by the canopy. In this way, $\Gamma_{scat}(f)$ can be written as $a(f)/2$. It is assumed that the single scattering albedo increases linearly and monotonically from 18 – 40 GHz, which is represented as

$$a(f) = c_o + c_1 f . \quad (7)$$

Once the surface temperature, T_v, is found by removing the atmospheric contribution from the SSM/I TBs, the apparent brightness temperature at any other frequency and incidence can be found if $TB_{UP}(f,\theta)$, $\tau(f)$, $TB_{down}(f)$ are known. These values are found from the SSM/I upwelling TBs determined from (4). The atmospheric upwelling brightness temperature at any other frequency and incidence (18 – 40 GHz, 0 – 55°) can be found using

$$Tup(f,\theta) = c_1 Fw(f,\theta)\left(T_{up}(22.235,53^o) - T_{up}(19.35,53^o)\right) + c_2 Fo(f,\theta)\left(T_{up}(37.0,53^o)\right) + c_3 f^2 \sec(\theta)$$

where

$$Fw(f,\theta) = \sec(\theta)\frac{\gamma}{fz} f^2\left[\frac{1}{(fz-f)^2+\gamma^2} + \frac{1}{(fz+f)^2+\gamma^2}\right]$$

$$Fo(f,\theta) = \sec(\theta)\gamma_o f^2\left[\frac{1}{(f-60)^2+\gamma_o^2} + \frac{1}{f^2+\gamma_o^2}\right] . \quad (8)$$

The first term in (8) is a measure of the shape and strength of the water vapor absorption line, f_z is 22.235 and f is in GHz. The third term is a measure of the absorption continuum and the second term is a measure of the shape and strength of the 60 GHz oxygen absorption line [6]. The hemispherical downwelling component is determined using the same form as (8), with the sec(θ) terms removed. The integrated optical depth is found using (5) with the upwelling TBs determined from (8). Once $TB_{up}(f,\theta)$, $\tau(f)$, $TB_{down}(f)$, are determined, (3) is used with the T_v determined from SSM/I to find the apparent TB at any other frequency and incidence from 18 - 40 GHz and 0 - 55° incidence. These values are the hot calibration reference temperatures for suitable regions in the Amazon rainforest.

III. Model Parameterizations

To determine the coefficients in the above equations, radiosonde data in the vicinity of the selected regions is used to model the apparent TBs, integrated optical depth, effective radiating temperature, and the upwelling and downwelling TBs. RaOb sounding data from October 2001 through September 2002 is used from four stations in the Amazon. The radiosonde data is acquired from NOAA's Forecast Systems Laboratory (FSL) radiosonde database. A plane parallel radiative transfer model is used with an updated version of the Liebe 1987 [7] atmospheric water vapor absorption model and the Rosenkranz 1993 [8] oxygen absorption model to determine the brightness temperature from the RaOb profiles.

The measured apparent TB data set consists of measurements from October 2001 through September 2002 from the DMSP SSM/I F13, F14, and F15 platforms acquired from Remote Sensing Systems. Two regions are chosen where the average magnitude of the V-pol – H-pol TBs is less than one for the 19.35 and 37.0 GHz channels. In this way, the emission from the regions is modeled as (2). Region 1 is 5° – 10° S and 65 ° – 74 ° W and region 2 is 1 ° S – 4° N and 53 ° – 59 ° W.

The equations in section II are parameterized using least-squares optimization of the modeled radiosonde database. The dependence of the single scattering albedo on frequency, (7), is determined by solving for *a(f)* in (3) using average modeled values for the atmospheric TB components with average SSM/I apparent TBs at 19,22, and 37 GHz.

The hot reference temperature is determined from 18 - 40 GHz and 0 – 55^o incidence from the parameterizations of the equations in II. Fig. 1 and Fig. 2 show the hot reference temperature versus frequency and incidence averaged over local time and time of year. A microwave radiometer operating within this range can use these reference temperatures for the TB calibration at the hot end of the TB spectrum.

IV. CONCLUSIONS

Satellite microwave radiometers require precisely calibrated brightness temperatures for the accurate retrieval of geophysical parameters. The on-orbit calibration of brightness temperature involves calibrating the TBs at the hottest and coldest ends of the TB dynamic range. Equations are developed to determine apparent brightness temperatures at other frequencies and incidence using SSM/I TBs. The equations are parameterized from 18 – 40 GHz and 0 – 55^o incidence using a radiative transfer model with RaOb profiles in the Amazon. In this way, a hot reference temperature is determined over regions of optically thick vegetation in the Amazon rainforest for the on-orbit calibration of microwave radiometers operating within this range.

V. REFERENCES

[1] N. Grody, "Remote sensing of the atmosphere from satellites using microwave radiometery," in *Atmospheric Remote Sensing By Microwave Radiometery*, M. Janssen, Ed. New York: Wiley, 1993, ch 6.

[2] C. Ruf, "Detection of Calibration Drifts in Spaceborne Microwave Radiometers Using a Vicarious Cold Reference," IEEE Trans. On Geosci. Remote Sens, vol. 38, 1, Jan. 2000.

[3] F. Ulaby, R. Moore, and A. Fung, *Microwave Remote Sensing, Active and Passive. Volume II: Radar Remote Sensing and Surface Scattering and Emission Theory*. Dedham, MA: Artech House, 1982, pp. 887-894.

[4] S. Keihm, M. Janssen, and C. Ruf, "TOPEX/POSEIDON microwave radiometer (TMR), III, Wet troposphere reange correctoin algorithm and pre-luanch error budget," IEEE Trans. Geosci. Remote Sens., vol. 33, 1, pp. 147 – 160. Jan. 1995.

[5] E. Westwater, "Ground-based microwave remote sensing of meteorological variables," in *Atmospheric Remote Sensing By Microwave Radiometery*, M. Janssen, Ed. New York: Wiley, 1993, ch 4.

[6] F. Ulaby, R. Moore, and A. Fung, *Microwave Remote Sensing, Active and Passive. Volume I: Microwave Remote Sensing Fundamentals and Radiometry*. Dedham, MA: Artech House, 1981, Ch. 5.

[7] S. Cruz Pol, C. Ruf, and S. Keihm, "Improved 20-32 GHz atmospheric absoption model," Radio Sci., vol 22, 5, pp. 1319-1333, 1998.

[8] P. Rosenkranz, "Abosrption of Microwaves by Atmospheric Gases," Atmospheric Remote Sensing by Microwave Radiometery, Chapter 2 Ed. By Janssen, Wiley, New York, 1993.

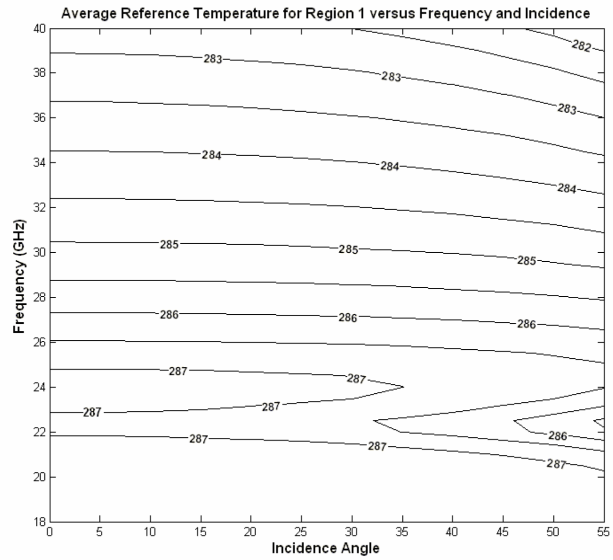

Figure 1. Hot Reference Temperature versus Frequency and Incidence Angle for Region 1, averaged over time of day and time of year. The contours are in half-degree increments.

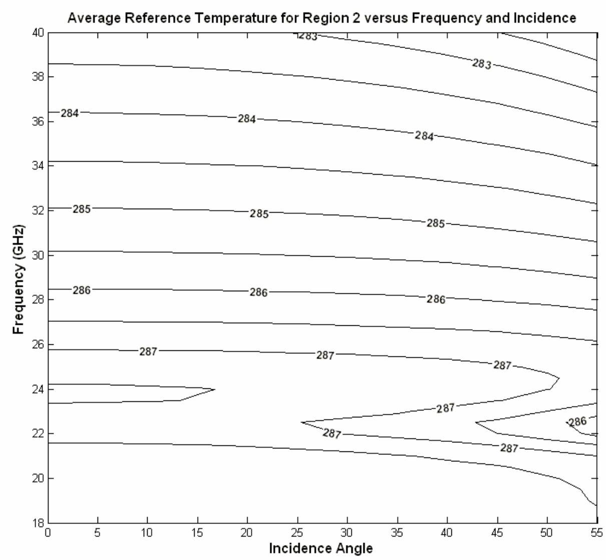

Figure 2. Hot Reference Temperature versus Frequency and Incidence Angle for Region 2, averaged over time of day and time of year. The contours are in half-degree increments.